Free falling inside flattened spheroids: Gravity tunnels with no exit

Richard Taillet

Citation: American Journal of Physics **86**, 924 (2018); doi: 10.1119/1.5075716
View online: https://doi.org/10.1119/1.5075716
View Table of Contents: http://aapt.scitation.org/toc/ajp/86/12
Published by the American Association of Physics Teachers

Free falling inside flattened spheroids: Gravity tunnels with no exit

Richard Taillet[a)]
Univ. Grenoble Alpes, USMB, CNRS, LAPTh, F-74940 Annecy, France

(Received 4 May 2018; accepted 7 October 2018)

A "gravity tunnel" is the name given to a fictitious deep shaft drilled inside the Earth so that objects dropped from the surface of the Earth would free fall without ever touching the walls. It is well known that because of the rotation of the Earth, such tunnels are not straight lines but instead they emerge westward of the antipodal point, when the Earth is approximated as a rotating sphere. In this article, we determine the shape of gravity tunnels by taking into account the polar flattening of the Earth resulting from its rotation. The Earth is described as a McLaurin spheroid, an exact equilibrium shape for a rotating homogeneous deformable body that provides a fair description of the actual shape of the Earth. It turns out that the gravitational force acting on an object located inside the spheroid has a simple form (it is harmonic), so that it is straightforward to compute analytically the free fall trajectories. This study follows a procedure presented several times in this journal and elsewhere, i.e., the trajectory is first computed in the geocentric (non-rotating) frame, and it is then analysed in the terrestrial (rotating) frame. We find that when the flattening of the Earth is taken into account, gravity tunnels have no exit: an object dropped from a point of the surface (other than on the equator or a pole) never reaches the surface again, unless the flattening has very specific (and unnatural) values. We also compute the deviations from the vertical for short falls and compare them to standard eastwards and southwards deviation expressions obtained with other modelizations of the gravity of the rotating Earth, in particular, for a rotating spherical body.

https://doi.org/10.1119/1.5075716

I. INTRODUCTION

When an object is dropped in a deep shaft from the surface of the Earth, its free fall trajectory is deviated eastwards and towards the equator (southwards if dropped from the northern hemisphere, as will be assumed throughout for the sake of simplicity) because of the rotation of the Earth. Several experiments have been set up to detect and to measure such deviations.[1–4] Some have led to positive detections of the eastwards component but no precise measurement has ever been made. On a more academic side, the theoretical determination of these deviations is often used in physics lessons to illustrate the effect of centrifugal and Coriolis forces, when the problem is analysed in the rotating terrestrial frame, modelling Earth as a spherical rotating body and discarding the friction with air (this last assumption will be made throughout in this paper). Analytical expressions can be obtained for these deviations, in particular, in the limit of short shafts. This problem can also be analysed in the geocentric non-rotating frame.[5,7–13] The free fall can be tracked for arbitrary long shafts up to the point where the object reaches the antipode, or more precisely reaches a point located westward of the antipode. The shafts following these trajectories, the object never making contact with the walls, are commonly referred as "gravity tunnels."[14]

One must be careful with the determination of the southwards deviation as it requires the proper definition of the local vertical direction at the drop point, in order to avoid any ambiguity about what is called "southward" or "northward." A natural definition of the vertical is the direction of a hanging plumbline which is stationary in the rotating frame. Because of the centrifugal force due to the Earth rotation, vertical differs from the radial direction (see Fig. 1). The plumbline is tilted towards the equator, and to be qualified as southwards (in the northern hemisphere), a free fall trajectory has to be even more tilted towards the equator than the plumbline.

The fact that the vertical is not perpendicular to the ground, on the surface of a rotating spherical body, can be confusing and is contrary to what can be verified experimentally on our planet. This is because our planet is not a sphere. As a deformable body, it is flattened at the poles by its rotation. The question of the exact equilibrium shape of a rotating deformable body has a long and rich history.[15,16] For a fluid body, this shape must be such that the weight at every point of the surface is perpendicular to the surface (were it not the case, the fluid would be set into motion and flow along the slope). In this work, we use classical results about the equilibrium shape of rotating deformable bodies to compute the shape of gravity tunnels inside a flattened rotating body. Once the classical results about gravity fields inside spheroids are given, the treatment is actually simple enough to be presented to college students in a physics curriculum. We find that inside flattened spheroids, gravity tunnels have only one free end; once released from the top of the shaft, the object follows an open infinite trajectory that never reaches the surface again. We also determine the shape of hanging plumblines, in order to derive the eastwards and southwards deviation of these tunnels. We finally compare our results to classical results obtained with different modelizations of the situation, in particular, to the case of a rotating spherical planet.

II. MCLAURIN SPHEROID

In the rotating frame, a deformable rotating body is in equilibrium when the effective force field (gravitational plus centrifugal) is orthogonal to the surface. The gravitational field is determined by the overall shape of the body and one must find shape-potential pairs that satisfy the condition above. Several such pairs have been proposed for a homogeneous body (mass

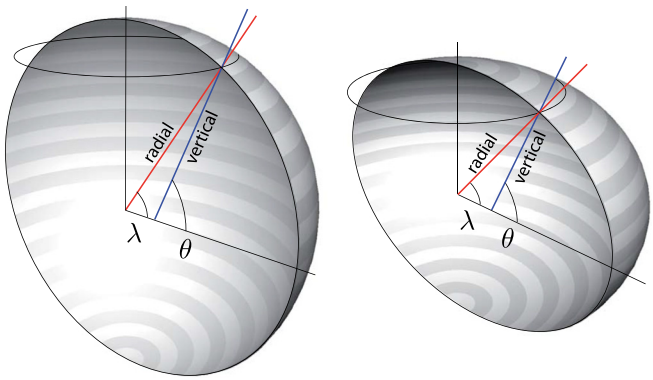

Fig. 1. Definition of the directions used for reference to evaluate the southwards deviation. The radial direction is orthogonal to the ground in the spherical case (left), but the vertical direction (defined as the straight line having the direction of the weight at the drop point) is not. The converse is true in the spheroidal case (right). The angles λ and θ are called geocentric latitude and geodesic latitude, respectively.

density ρ is uniform inside the body). Colin McLaurin showed in 1742 that axisymmetric spheroidal bodies flattened at the pole subject to a global "solid body" rotation can satisfy this condition, provided that their rotation rate Ω is related to the ellipticity e of the spheroid by the condition given below, see Eq. (4). This is possible only if Ω is lower than some critical value Ω_m (see below), a condition well verified by the Earth. This is called a McLaurin spheroid. Later in history, it was shown that instabilities can develop at rotation rates higher than Ω_m or, even for low Ω, at high values of the ellipticity. Other shapes must then be considered,[17] such as Jacobi ellipsoids, which are not axisymmetric, Riemann ellipsoids, with interior differential rotation, and Poincaré pear-shaped geoids. In this article, the gravitating body is described as a McLaurin spheroid that provides a fair description of the shape of the Earth.

In the geocentric frame (see Fig. 2), where coordinates are denoted (x, y, z), the equation of the surface of a spheroid is

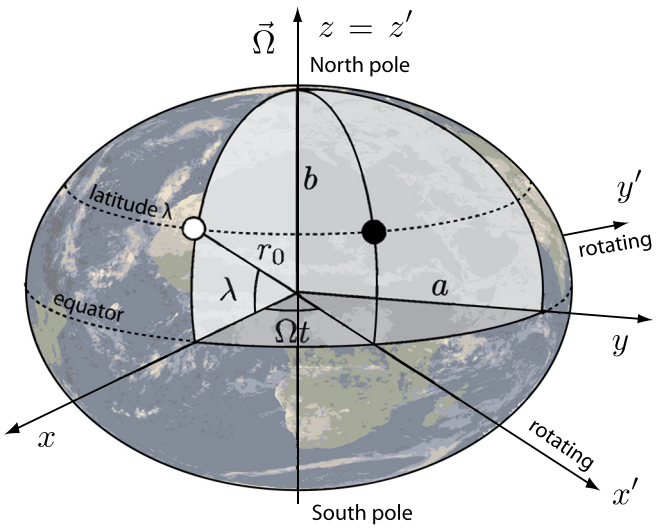

Fig. 2. Definition of the (x, y, z) coordinates in the geocentric (non-rotating) frame and the (x', y', z') coordinates in the terrestrial frame, rotating at angular velocity Ω. Also shown are the semi-major axis a and semi-minor axis b of the meridian ellipse. Ellipticity has been strongly exaggerated relative to the Earth value. The white dot indicates the position of the drop point at initial time and the black circle indicates the position of the drop point at time t.

$$\frac{x^2}{a^2}+\frac{y^2}{a^2}+\frac{z^2}{b^2}=1, \tag{1}$$

where a and b, respectively, denote the semi-major axis and the semi-minor axis of the meridian ellipse. They are related through the ellipticity or eccentricity e, defined such that $b=a\sqrt{1-e^2}$ ($e=0$ for a sphere and $e\approx 0.082$ for our Earth[18]). A remarkable property of homogenous spheroids is that the gravitational field inside the spheroid has a harmonic form. For an axisymmetric spheroid (see the Appendix for demonstrations),

$$\vec{g}=\begin{pmatrix}-\omega_1^2 x\\ -\omega_1^2 y\\ -\omega_2^2 z\end{pmatrix}, \tag{2}$$

where

$$\begin{cases}\omega_1^2\equiv\dfrac{3}{2}\omega^2\left(\dfrac{\sqrt{1-e^2}}{e^3}\operatorname{asin} e-\dfrac{1-e^2}{e^2}\right)\approx\omega^2-\dfrac{1}{5}e^2\omega^2\\ \omega_2^2\equiv\dfrac{3}{2}\omega^2\left(\dfrac{2}{e^2}-\dfrac{2\sqrt{1-e^2}}{e^3}\operatorname{asin} e\right)\approx\omega^2+\dfrac{2}{5}e^2\omega^2,\end{cases} \tag{3}$$

where $\omega^2\equiv 4\pi G\rho/3$ and G is the Newton constant. (In Eq. (3), we give the exact form as well as a first-order approximation when $e\ll 1$, the exact form being used in the rest of this work.) These quantities are shown in Fig. 3 as functions of e. With the terrestrial mean value $\rho_\oplus\approx 5.52\times 10^3\,\mathrm{kg\cdot m^{-3}}$, we obtain $\omega\approx 1.24\times 10^{-3}\,\mathrm{rad\cdot s^{-1}}$ and an associated period $T_\oplus=2\pi/\omega_\oplus\approx 84.3\,\mathrm{min}$. This spheroid describes the equilibrium shape of a rotating body if in the rotating frame, the total force field (gravitational plus centrifugal)

$$m\vec{g}-m\vec{a}_c=\begin{pmatrix}-m\omega_1^2 x\\ -m\omega_1^2 y\\ -m\omega_2^2 z\end{pmatrix}+\begin{pmatrix}m\Omega^2 x\\ m\Omega^2 y\\ 0\end{pmatrix}$$

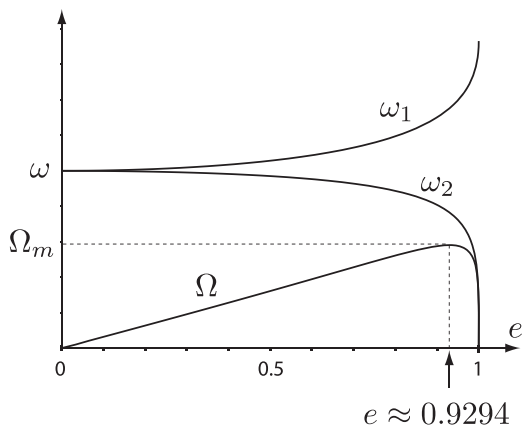

Fig. 3. The three pulsations ω_1, ω_2, and Ω relevant for the description of McLaurin spheroids. The angular velocity Ω of the object must be related to the two other quantities by Eq. (4) for the gravitating body to qualify as a McLaurin spheroid. This angular velocity has a maximum possible value Ω_m, obtained for the particular value of the ellipticity $e\approx 0.9294$.

is everywhere orthogonal to the surface. From the previous expression, it can be shown (see the Appendix) that this is indeed the case provided that

$$\Omega^2 = \omega_1^2 - \omega_2^2(1-e^2) \tag{4}$$

or

$$\Omega^2 = \frac{3}{2}\omega^2\left\{\frac{\sqrt{1-e^2}}{e^3}(3-2e^2)\operatorname{asin} e - \frac{3(1-e^2)}{e^2}\right\} \approx \frac{2}{5}\omega^2 e^2. \tag{5}$$

The ellipticity e is thus related to the ratio Ω/ω (the small e limit had been enunciated by Newton[15,16,19]). This ratio is shown in Fig. 3 as a function of e. As mentioned above, the rotation rate Ω must be lower than $\Omega_m \approx 0.58\omega$, a value obtained for $e \approx 0.9294$. To every rotation rate $\Omega < \Omega_{\mathrm{m}}$ correspond two possible values of e.

For a body having the same mass density as the Earth, $\Omega_m \approx 7.19 \times 10^{-4}\,\mathrm{rad\cdot s^{-1}}$ and the associated period is $T_m \approx 145\,\mathrm{min}$. The rotation rate of the Earth $\Omega_\oplus \approx 7.37 \times 10^{-5}\,\mathrm{rad\cdot s^{-1}}$ is well below Ω_{m}. According to the previous equation, for a McLaurin spheroid rotating as the same angular velocity as the Earth, the two possible values of the ellipticity are $e \approx 0.99999887$ (very flattened spheroid) and $e \approx 0.094$ (slightly flattened). The latter value is close to, but significantly different from the value $e = 0.082$ measured for the spheroid best describing our Earth. The difference is partly due to the fact that Earth is not a homogeneous uniformly rotating body. However, we expect that modelling the Earth with a McLaurin spheroid provides an improvement over the spherical model, as it introduces a flattening that is consistently with the rotation rate. For the sake of curiosity, we will study the trajectories inside McLaurin spheroids of any ellipticity e (not necessarily small as in the case of Earth). For high values of e, we prevent the complications associated with the onset of instabilities in fluid bodies by assuming that the planet is a non-deformable rotating body described by a McLaurin spheroid. The rest of the paper is devoted to the study of gravity tunnels inside such spheroids. It would be straightforward to extend the following results to the case of spheroids rotating at an angular velocity different from the value given in Eq. (4). The vertical would then not be orthogonal to the ground.

III. FREE FALL TRAJECTORY

To describe the free fall of an object dropped from the surface of the spheroid into a gravity tunnel, it is simpler to first study the problem in the (non-rotating) geocentric frame. For a spherical body, this has been studied under different assumptions about the gravitational force acting on the falling body, some works[7,8] considering a $1/r^2$ gravitation law (describing the fall from a drop point above the ground), others[11] considering a harmonic force (describing the fall in shafts drilled inside the Earth, see below), others still[6] considering a gravitational force of constant magnitude (an approximation valid for very short falls). In this section, we turn to the spheroid case and study the fall in the non rotating frame.

In the geocentric frame, when no friction with air is present, the falling body is only subject to the purely gravitational force given in Eq. (2) (no centrifuge force). The equations of motion are

$$\begin{cases} \ddot{x} + \omega_1^2 x = 0 \\ \ddot{y} + \omega_1^2 y = 0 \\ \ddot{z} + \omega_2^2 z = 0. \end{cases} \tag{6}$$

These are the equations of independent harmonic oscillators, with a period along z that is different (shorter) than the period in the xy plane.

The object is dropped at $t = 0$ from a point of geocentric latitude λ, defined in Fig. 2, so that the initial values of the coordinates are

$$x_0 = r_0\cos\lambda, \quad y_0 = 0 \quad \text{and} \quad z_0 = r_0\sin\lambda, \tag{7}$$

where r_0 denotes the initial distance between the body and the center of the Earth, obtained from Eq. (1) to be

$$r_0 = \frac{a\sqrt{1-e^2}}{\sqrt{1-e^2\cos^2\lambda}}. \tag{8}$$

In the geocentric frame, the initial velocity is $(\dot{x}, \dot{y}, \dot{z}) = (0, r_0\Omega\cos\lambda, 0)$. Integration of Eq. (6) yields

$$\begin{cases} x(t)/r_0 = \cos\lambda\cos\omega_1 t \\ y(t)/r_0 = \alpha\cos\lambda\sin\omega_1 t \\ z(t)/r_0 = \sin\lambda\cos\omega_2 t, \end{cases} \tag{9}$$

where we have defined $\alpha \equiv \Omega/\omega_1$, a quantity close to 1/17 for the Earth. An example of a trajectory in the geocentric frame is shown in Fig. 4.

Denoting with primes the quantities relative to the (rotating) terrestrial frame (see Fig. 2), the unit vectors of the rotating and non-rotating frames are related by

$$\begin{cases} \vec{e}_x = \cos\Omega t\,\vec{e}'_x - \sin\Omega t\,\vec{e}'_y \\ \vec{e}_y = \sin\Omega t\,\vec{e}'_x + \cos\Omega t\,\vec{e}'_y \\ \vec{e}_z = \vec{e}'_z \end{cases} \tag{10}$$

so that the trajectory in the terrestrial frame is described by

$$\begin{cases} x'(t)/r_0 = \cos\lambda\cos(\omega_1 t)\cos(\Omega t) \\ \qquad\qquad + \alpha\cos\lambda\sin(\omega_1 t)\sin(\Omega t) \\ y'(t)/r_0 = \alpha\cos\lambda\sin(\omega_1 t)\cos(\Omega t) \\ \qquad\qquad - \cos\lambda\cos(\omega_1 t)\sin(\Omega t) \\ z'(t)/r_0 = \sin\lambda\cos(\omega_2 t). \end{cases} \tag{11}$$

This gives the exact equation, in parametric form, for gravity tunnels inside McLaurin spheroids. The shape of these tunnels is shown in Fig. 5. The value of the eccentricity ($e = 0.8$) has been chosen much higher than the value corresponding to our Earth ($e \approx 0.082$), in order to make the features clearly visible. Contrary to the case usually studied of a rotating spherical Earth, the falling object, once dropped, does not reach the surface again, unless the ratio ω_1/ω_2 is rational

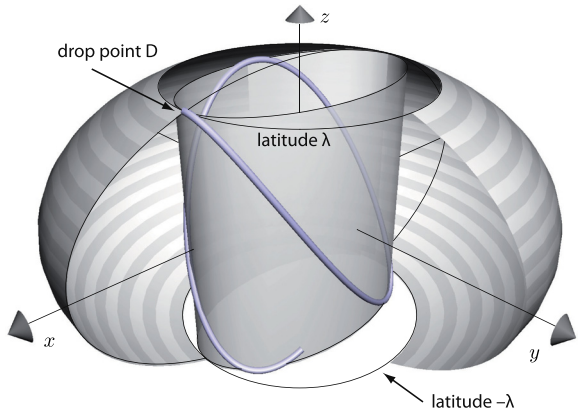

Fig. 4. In the geocentric (non-rotating) frame, the object dropped by an experimenter set on the surface of the Earth has an initial velocity tangential to the circle of latitude λ. The free fall trajectory (drawn as a tube) is a sine curve imprinted on an elliptical cylinder (transparent inner cylinder on the figure) with a minor to major axes ratio α (see text). We have chosen a high value for the ellipticity ($e = 0.8$) to show clearly the features of the trajectory. The period along the polar axis is different from the period in the equatorial plane. If the ratio of these periods is not a rational number, then the trajectory never reaches the circles of latitude λ and $-\lambda$, i.e., the dropped object never reaches the surface again.

(which requires a very peculiar and unnatural numerical choice for e and Ω). This is best seen in the geocentric frame (see Fig. 4). Gravity tunnels are not tunnels in the end, but wander endlessly inside the Earth. This is not necessarily a problem for potential future gravity tunnel builders, as for the numerical values relevant to describe our Earth ($e = 0.082$), the first turning point of the tunnel is located only about 30 m under ground (for a latitude $\lambda = 45°$).

It is worth mentioning, in particular, when addressing students, that the free fall trajectory can be straightforwardly plotted with software freely available on most modern computers. In the Supplementary material, a code in python is provided to reproduce Figs. 4 and 5, for any value of e. The plots can be rotated interactively, to get a better feeling of the 3D shape.[22]

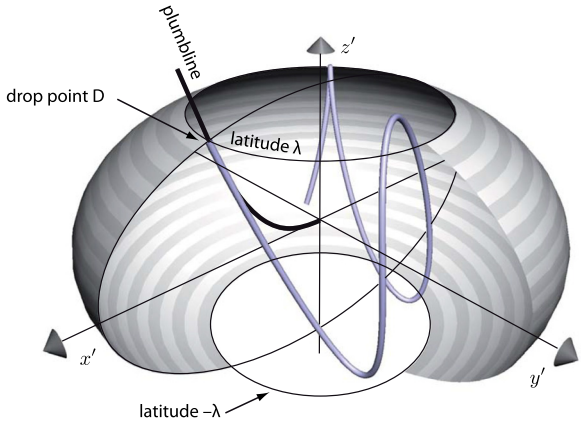

Fig. 5. Shapes of gravity tunnels (tube) and plumbline (thick black line) inside a rotating spheroidal body, in the terrestrial (rotating) frame, with the same value of e as in the previous figure. Only part of the surface of the body has been drawn, to allow visualization of the inside. Note that the rotating bodies are not hollow, but are filled with a uniform mass density ρ. The whole tunnel is located inside the cylinder delimited by the two circles at latitudes $\pm\lambda$.

IV. VERTICALITY AND SHAPE OF THE PLUMBLINE

The shape of gravity tunnels is completely determined by the set of Eqs. (11). It is useful to present the free fall trajectory in a different way, examining the departure of the free fall from verticality, in order to compare with classical results used to analyse the results of experiments performed in deep shafts. This requires a careful definition of verticality[9,20] and this section is devoted to such a definition.

From the experimental point of view, the best way to define verticality is to hang a plumbline from the drop point. This is actually the reference used in all experimental setups.[1–4] When a plumbline is at rest in the terrestrial frame, its shape follows the effective force field lines (gravitational plus centrifugal). In the case of the McLaurin spheroid, this shape, from Eq. (4), is

$$\frac{dx'}{dz'} = \frac{F_x}{F_z} = \frac{\Omega^2 - \omega_1^2}{-\omega_2^2}\frac{x'}{z'} = (1-e^2)\frac{x'}{z'} \tag{12}$$

so that, for the field line starting at position $(y, z) = (r_0 \cos\lambda, r_0 \sin\lambda)$,

$$\frac{x'}{r_0\cos\lambda} = \left(\frac{z'}{r_0\sin\lambda}\right)^{1-e^2}. \tag{13}$$

This is the equation of the field line defining the vertical direction everywhere in the spheroid. By definition of the McLaurin spheroids, the vertical is perpendicular to the ground, everywhere on the surface. The angle θ between the vertical and the x' direction, at the drop point, is called the geodesic latitude. It is given by

$$\tan\theta = \left.\frac{dz'}{dx'}\right|_{\text{drop}},$$

where the vertical displacements dx' and dz' are related by Eq. (12)

$$\frac{dx'}{x'} = (1-e^2)\frac{dz'}{z'}$$

so that the geocentric latitude λ and the geodesic latitude θ are related through

$$\tan\theta = \frac{1}{1-e^2}\frac{z'}{x'} = \frac{\tan\lambda}{1-e^2}. \tag{14}$$

Ideally, one would like to track the successive positions along the trajectory with a curvilinear system of coordinates, one coordinate along the plumbline, the two others locally perpendicular to it. It turns out that the price in complexity is not worth the trouble: it is simpler to describe both the shape of the plumbline and the trajectory of the falling body in a well-chosen Cartesian frame. More specifically, we set the Z axis along the direction of the tangent to the plumbline (the local vertical), a E axis towards the east and a S axis to complete the orthogonal reference frame (see Fig. 6). We will call it the "vertical stick" frame. Some authors define still another reference frame (labeled "radial stick" in the figure), with Z along the radial direction. This choice may lead to confusion and will not be considered here.

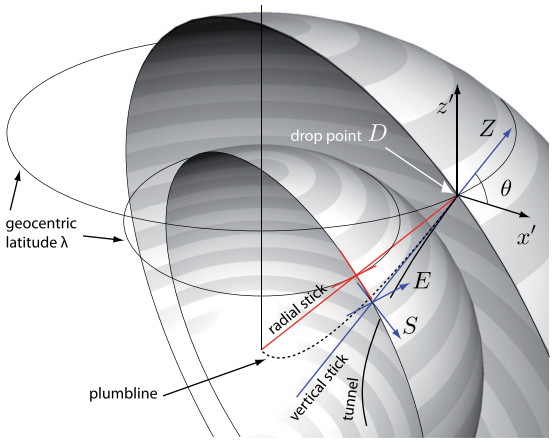

Fig. 6. Definition of the directions used for reference to evaluate the eastwards and southwards deviations. The outer surface is the surface of the planet and the inner surface has been drawn to help visualize the relative position of the other elements in the figure. The radial direction is orthogonal to the ground in the spherical case, but not the vertical direction (defined as the straight line having the direction of $\vec{g}$ at the drop point). In the spheroidal case, the vertical direction is orthogonal to the ground at the drop point D. The dashed line is the plumbline hanging from D. It is contained within the meridional plane passing through D, together with the radial stick and the vertical stick.

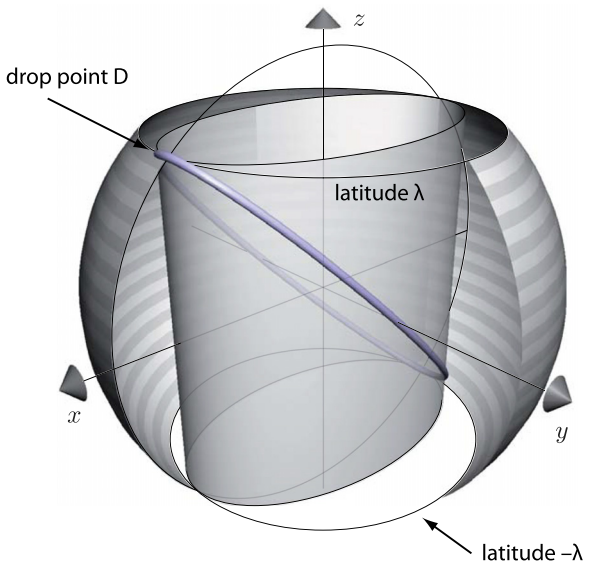

Fig. 7. Free fall trajectory in the geocentric (non-rotating) frame, for a spherical planet. As in the previous figure, only part of the surface of the body has been drawn. The body is released from the drop point with a velocity $R\Omega\cos\lambda$ that is tangential to the parallel at latitude λ. The trajectory is an ellipse, centered on the center of the planet. Every half oscillation, the body reaches the latitude $\pm\,\lambda$ at the surface of the planet. This figure can be compared to Fig. 4, obtained in the case of a McLaurin spheroid.

V. THE ROTATING SPHERE

Before we compute the deviations from the vertical, we present the trajectories that are obtained when the Earth is modelled as a homogeneous rotating sphere, in order to compare them to the McLaurin spheroid model presented above. This is not the low-Ω or low-e limit of the previous model, as a McLaurin spheroid with $e=0$ must be non-rotating. Inside a spherical body, the gravitational field is radial, $\vec{g}=-\omega^2\vec{r}$. Using the procedure presented in Sec. III, we find

$$\begin{cases} x(t)/R = \cos\lambda\cos\omega t \\ y(t)/R = \alpha\cos\lambda\sin\omega t \\ z(t)/R = \sin\lambda\cos\omega t \end{cases} \tag{15}$$

in the geocentric frame, where $\alpha\equiv\Omega/\omega$ is defined as before. The trajectory is shown in Fig. 7. In the terrestrial frame, the trajectory is

$$\begin{cases} x'(t)/R = \cos\lambda\cos(\omega t)\cos(\alpha\omega t) \\ \qquad\qquad + \alpha\cos\lambda\sin(\omega t)\sin(\alpha\omega t) \\ y'(t)/R = \alpha\cos\lambda\sin(\omega t)\cos(\alpha\omega t) \\ \qquad\qquad - \cos\lambda\cos(\omega t)\sin(\alpha\omega t) \\ z'(t)/R = \sin\lambda\cos(\omega t) \end{cases} \tag{16}$$

and is shown in Fig. 8. In this case, gravity tunnels have multiple exits, the falling object reaching the surface every half-period of the ωt oscillation.

For future reference, the shape of the plumbline can be computed exactly as above, in the case of a rotating sphere. One finds

$$\frac{x'}{R\cos\lambda} = \left(\frac{z'}{R\sin\lambda}\right)^{1-\alpha^2}, \tag{17}$$

and the relation between the geocentric latitude λ and the geodesic latitude θ becomes

$$\tan\theta = \frac{\tan\lambda}{1-\alpha^2}. \tag{18}$$

The shape of gravity tunnels inside rotating spheres has been described in Ref. 11. They use a different coordinates system and it is not illuminating to compare our expressions to theirs. For instance, they define an angular eastwards coordinate as the difference of longitude between the drop point and the current position. Using their expressions, the y' coordinate along the fall is given by

$$\frac{y'}{R} = \cos\lambda\sin\left\{\left[(1-\alpha)\omega t + \arctan\left(\frac{(\alpha-1)\sin\omega t\cos\omega t}{1+(\alpha-1)\sin^2\omega t}\right)\right] \times\sqrt{1-(1-\alpha^2)\sin^2\omega t}\right\}, \tag{19}$$

where notations have been adapted to match those used here. This can be compared to our expression (16)

$$\frac{y'}{R} = \alpha\cos\lambda\sin(\omega t)\cos(\alpha\omega t) - \cos\lambda\cos(\omega t)\sin(\alpha\omega t). \tag{16}$$

It is not obvious, but true, that Eqs. (19) and (16) are exactly equivalent for all values of α.

VI. EASTWARD AND SOUTHWARD DEVIATIONS

In this section, we give exact expressions for the eastwards and the southwards component of the deviation from

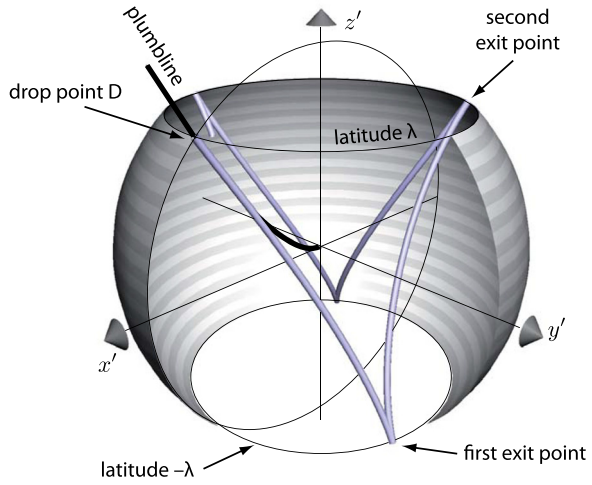

Fig. 8. Shapes of gravity tunnels and plumbline inside a rotating spherical body. As in the previous figure, only part of the surface of the body has been drawn. The thick black line shows the shape of the plumbline hanging from the drop point D. The tunnel deviates from the vertical direction towards the east and towards the south (below the plumbline in the figure). Moreover, in this case, the gravity tunnels have an infinite numbers of exits, corresponding to every half period of the ωt oscillation in the three x, y and z directions. This figure can be compared to Fig. 5, obtained in the case of a McLaurin spheroid.

verticality, inside McLaurin spheroids, in the frame defined by the vertical stick defined in Sec. IV. As all the experiments involve relatively small fall heights, corresponding to $\omega t \ll 1$ (and $\Omega t \ll 1$), we also provide the corresponding expressions obtained the small time limit. We finally compare them to classical results obtained for the case of a rotating sphere instead of the McLaurin spheroid.

In the vertical stick frame, the coordinates of the falling object are

$$\begin{cases} S = \Delta x' \sin\theta - \Delta z' \cos\theta \\ E = y' \\ Z = \Delta x' \cos\theta + \Delta z' \sin\theta, \end{cases} \tag{20}$$

where θ is the geodesic latitude of the drop point and $\Delta x' = x' - x'_d$ and $\Delta z' = z' - z'_d$, with $x'_d = r_0 \cos\lambda$ and $z'_d = r_0 \sin\lambda$, are the coordinates of the drop point in the terrestrial frame.

A. McLaurin spheroid

For the McLaurin spheroid, inserting Eq. (11) into Eq. (20), one computes S and E to be

$$\begin{cases} S/r_0 = \sin\theta\cos\lambda(\cos(\omega_1 t)\cos(\Omega t) \\ \qquad + \alpha\sin(\omega_1 t)\sin(\Omega t) - 1) \\ \qquad - \cos\theta\sin\lambda(\cos(\omega_2 t) - 1) \\ E/r_0 = \alpha\cos\lambda\sin(\omega_1 t)\cos(\Omega t) \\ \qquad - \cos\lambda\cos(\omega_1 t)\sin(\Omega t). \end{cases} \tag{21}$$

These functions of time depend on the latitude of the drop point and on the ellipticity e. The small time limit of E and S can be obtained by a Taylor expansion of these expressions. It is also interesting to start the expansion a step sooner in the computation, to facilitate any comparison with other works in which the approximations are made at the start. For short times, the Taylor expansion of expressions (11) at order t^4 yields

$$\begin{cases} x' \approx r_0\cos\lambda\left[1 + \left(\dfrac{\Omega^2 - \omega_1^2}{2}\right)t^2 \right. \\ \qquad \left. -\dfrac{1}{8}\left(\Omega^2 - \omega_1^2\right)\left(\Omega^2 + \dfrac{\omega_1^2}{3}\right)t^4\right] \\ y' \approx r_0\dfrac{\Omega\cos\lambda}{3}\left(\omega_1^2 - \Omega^2\right)t^3 \\ z' \approx r_0\sin\lambda\left(1 - \dfrac{\omega_2^2 t^2}{2} + \dfrac{\omega_2^4 t^4}{24}\right), \end{cases}$$

where there are no assumption on Ω or ω, and where we have used the definition of α, so that $\alpha\omega_1 = \Omega$. Taking the origin at the drop point, we have

$$\begin{cases} \Delta x' \approx r_0\cos\lambda\left[\left(\dfrac{\Omega^2 - \omega_1^2}{2}\right)t^2 \right. \\ \qquad \left. -\dfrac{1}{8}\left(\Omega^2 - \omega_1^2\right)\left(\Omega^2 + \dfrac{\omega_1^2}{3}\right)t^4\right] \\ \Delta y' \approx r_0\dfrac{\Omega\cos\lambda}{3}\left(\omega_1^2 - \Omega^2\right)t^3 \\ \Delta z' \approx r_0\sin\lambda\left(-\dfrac{\omega_2^2 t^2}{2} + \dfrac{\omega_2^4 t^4}{24}\right). \end{cases}$$

Finally, inserting into Eq. (20), using Eqs. (4) and (14), and keeping only the lowest nonvanishing order in t, we find

$$\begin{cases} S \approx \dfrac{1}{24} r_0 \sin\lambda\cos\theta\,\omega_2^2 t^4\left[4\Omega^2 - e^2\omega_2^2\right] \\ E \approx \dfrac{1}{3} r_0 \Omega\cos\lambda\left(\omega_1^2 - \Omega^2\right)t^3 \\ Z \approx -\dfrac{1}{2} r_0 \dfrac{\sin\lambda}{\sin\theta}\omega_2^2 t^2. \end{cases} \tag{22}$$

These expressions give the eastwards and equatorwards deviations relative to the "vertical stick" defined above. They are valid for small times, but no assumption is made regarding the value of e. The E component is always positive at small times, whatever the position of the drop point and the value of the ellipticity e, i.e., the body always starts with a slight deviation towards east. This can be understood as a direct consequence of the conservation of angular momentum, or equivalently of the Kepler's law of areas.[5,6] The situation is less simple for the S component. The quantity $4\Omega^2 - e^2\omega_2^2$ changes signs for $e = e_0 \approx 0.887732$. The S component is positive at small times when $e < e_0$ (this is the case of the ellipticity of Earth) and is negative at small times when $e > e_0$, i.e., the body deviates slightly northwards of the vertical stick chosen as a reference (see Fig. 9). However, as we show below, even in these cases the trajectory is always

located south of the plumbline at small times. This is to be expected, as a body falling with a vanishingly small velocity would follow the plumbline, whereas the object in free fall acquires a finite velocity and is carried away from the plumbline by inertia. The body deviates to the side of the plumbline opposite to its curvature center, i.e., southwards in the northern hemisphere.

Since the value of e is low for Earth, it is interesting to consider the limit $e \to 0$ of these expressions. We then have $e^2\omega_2^2 \approx 5\Omega^2/2 \to 0$ and, at lowest order in Ω, $r_0 \to R$ so that, with $g \equiv R\omega^2$,

$$\begin{cases} S \approx \dfrac{1}{16} R\Omega^2 \cos\lambda \sin\lambda\, g t^4 \\ E \approx \dfrac{1}{3}\Omega \cos\lambda\, g t^3 \\ Z \approx -\dfrac{1}{2} g t^2. \end{cases} \tag{23}$$

The deviations can be written as a function of fall height

$$\begin{cases} S \approx \dfrac{1}{10} R\Omega^2 \cos\lambda \sin\lambda \dfrac{Z^2}{g} \\ E \approx \dfrac{2}{3}\Omega \cos\lambda \sqrt{\dfrac{2Z}{g}}. \end{cases} \tag{24}$$

B. Comparison with other models

In the literature, one can find similar expressions obtained by other approaches. For instance, in the classical treatment taught in introductory mechanics, the norm and direction of weight (gravitational attraction and centrifugal force) are supposed to be independent of location in the terrestrial frame. They define the direction of the z axis (it is not radial). The equations of motion in the terrestrial frame involve centrifugal and Coriolis forces. Their integration yields, at the lowest order in t, the classical result

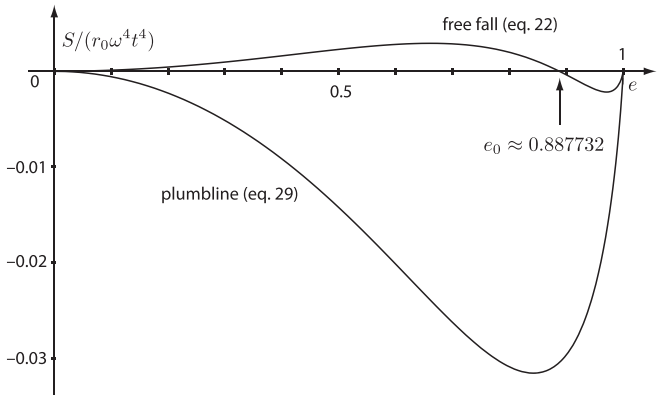

Fig. 9. Evolution of the deviation of the trajectory and of the plumbline along S for short times, both relative to the vertical stick, with the ellipticity e. The graph represents $S/r_0\omega^4 t^4$ to ease the comparison of the Taylors expansions of these two quantities at short times. No assumption is made on the magnitude of e. For $e > e_0$, the trajectory is deviated northwards (in the northern hemisphere) of the vertical stick. However, it is always deviated southwards of the plumbline.

$$\begin{cases} S \approx \dfrac{1}{6} R\Omega^2 \cos\lambda \sin\lambda\, g t^4 \\ E \approx \dfrac{1}{3}\Omega \cos\lambda\, g t^3. \end{cases} \tag{25}$$

The eastwards deviation is the same as in Eq (23). This is to be expected, as at this order it is entirely due to the Coriolis acceleration during a fall obeying $z = -gt^2/2$. On the other hand, the southwards component is different in the two approaches. Indeed, this quantity is sensitive to several effects: one contribution is the effect of the Coriolis acceleration due to the (small) eastwards velocity (precisely the one leading to E), others include the spatial dependence of the weight (see Ref. 9). For instance, when the object is dropped above the ground, and is attracted by the Earth with a $1/r^2$ law, the eastwards deviation at small times is the same as before but the southwards deviation, for small rotation rates Ω, is given by

$$S \approx \frac{3R\Omega^2}{4} \cos\lambda \sin\lambda\, g t^4. \tag{26}$$

(See Refs. 8 and 9 for the method, adapted here to use the vertical direction as a reference.) Finally, the result for gravity tunnels inside a rotating spherical body can be obtained by the same method as for the spheroid. The Taylor expansion of Eq. (16) for $\omega t \ll 1$ at order t^4 (no assumption on α) yields

$$\begin{cases} x'/R \approx \cos\lambda \left(1 - \dfrac{1}{2}(1-\alpha^2)\omega^2 t^2 \right. \\ \qquad\qquad \left. + \dfrac{1}{24}(1-\alpha^2)(1+3\alpha^2)\omega^4 t^4 \right) \\ y'/R \approx \dfrac{1}{3} R \cos\lambda\, \omega^3 t^3 \\ z'/R \approx \sin\lambda \left(1 - \dfrac{1}{2}\omega^2 t^2 + \dfrac{1}{24}\omega^4 t^4 \right). \end{cases} \tag{27}$$

Using Eqs. (20) and (18), keeping only the lowest orders in the final result, and using $g = R\omega^2$, we then find

$$\begin{cases} S \approx \dfrac{1}{8} R\Omega^2 \cos\theta \sin\lambda\, g t^4 \\ E \approx \dfrac{1}{3}\Omega \cos\lambda\, g t^3 \\ Z \approx -\dfrac{1}{2}\dfrac{\sin\lambda}{\sin\theta}\, g t^2. \end{cases} \tag{28}$$

This is the small time expansion with no assumption on the magnitude of Ω. Here again, the eastwards deviation is the same as in Eq. (23) but the southwards deviation has still another expression: even though the rotating sphere and the McLaurin spheroid have a common $\Omega \to 0$ limit (a non rotating sphere), for any small but finite value of Ω, the two models are physically different, with distinct spatial dependences of the weight, hence different southwards deviations.

C. Deviation of the plumbline

The expressions Eqs. (21) and (22) above give the equation of the trajectory in the vertical stick frame defined in

Sec. IV. To compute the deviation with respect to the plumbline, we must also compute the equation of the plumbline in the vertical stick frame. Along the plumbline, the (x', z') coordinates are related to the (Z_p, Y_p) coordinates through

$$\begin{cases} \Delta x' = Z_p \cos\theta + S_p \sin\theta \\ \Delta z' = Z_p \sin\theta - S_p \cos\theta. \end{cases}$$

Substituting into Eq. (13), we obtain

$$\frac{Z_p \cos\theta}{r_0 \cos\lambda} + \frac{S_p \sin\theta}{r_0 \cos\lambda} = \left(1 + \frac{Z_p \sin\theta}{r_0 \sin\lambda} - \frac{S_p \cos\theta}{r_0 \sin\lambda}\right)^{1-e^2} - 1.$$

So far this expression is exact. Expanded for both $S_p \ll r_0$ and $Z_p \ll r_0$, it is

$$\frac{Z_p \cos\theta}{r_0 \cos\lambda} + \frac{S_p \sin\theta}{r_0 \cos\lambda} \approx (1-e^2)\frac{Z_p \sin\theta}{r_0 \sin\lambda} - (1-e^2)\frac{S_p \cos\theta}{r_0 \sin\lambda} - \frac{e^2(1-e^2)}{2}\left(\frac{Z_p \sin\theta}{r_0 \sin\lambda} - \frac{S_p \cos\theta}{r_0 \sin\lambda}\right)^2.$$

Using the relation Eq. (14), we find that the terms linear in Z_p cancel out (this is because Z truly is the vertical direction), indicating that S_p is at best proportional to Z_p^2, so that, gathering the remaining terms and using Eq. (14), we arrive at

$$\frac{S_p}{r_0 \cos\theta \sin\lambda} \approx -\frac{e^2}{2}\left(\frac{Z_p \sin\theta}{r_0 \sin\lambda}\right)^2.$$

In the limit of short falls, the deviation of the plumbline at the depth Z reached at time t is found using Eq. (22) to be

$$S_p \approx -\frac{e^2}{8} r_0 \cos\theta \sin\lambda\, \omega_2^4 t^4. \tag{29}$$

This is plotted as a function of e in Fig. 9. In the northern hemisphere, the plumbline is located north of the vertical stick used as a reference. The final expression for the deviation of the free fall relative to the plumbline, for short times t but arbitrary values of e, is thus obtained from Eqs. (22) and (29) to be

$$\Delta S = S - S_p \approx \frac{1}{12} r_0 \sin\lambda \cos\theta\, \omega_2^2 t^4 \left[2\Omega^2 + e^2\omega_2^2\right]. \tag{30}$$

The deviation is always positive, the free fall trajectory is always deviated southwards at short times when the object is dropped from the northern hemisphere.

In the small e limit, we have $e^2 \approx 5\Omega^2/2\omega^2$ and $\sin\theta \approx \sin\lambda$, and the previous expressions become

$$S_p \approx -\frac{5}{16} r_0 \cos\theta \sin\lambda\, \omega_2^4 t^4 \approx -\frac{5\Omega^2}{4}\cos\lambda \sin\lambda \frac{Z_p^2}{g}$$

$$\Delta S \approx \frac{3}{8} R \cos\lambda \sin\lambda\, \omega^4 t^4 \approx \frac{3\Omega^2}{2}\cos\lambda \sin\lambda \frac{Z^2}{g}.$$

This is a southwards deviation.

VII. CONCLUSION

The aim of this article is to present some results concerning the free fall of objects inside a rotating homogeneous flattened body, described as a McLaurin spheroid. From there, one could extend the study to triaxial homogeneous ellipsoids, the potential of which is still harmonic with three distinct pulsations ω_1, ω_2, and ω_3 associated with each symmetry axis. The analytical expressions for these quantities, as a function of e (the extension of Eq. (3) to the triaxial case) involve elliptic functions and are not so well suited to an introductory exposition. We have also computed the small t limit of the exact equations and found a new expression for the southwards deviation, when the flattening of Earth is taken into account. This study can be introduced early in a physics curriculum, using only elementary results about harmonic oscillators and rotating frames, along with the statements of the properties of the McLaurin spheroid presented in this article. It can complement a lecture on inertial forces and non-Galilean reference frames, to help students understand the nature of these forces in a situation where the trajectory can be computed exactly, and more easily than in the Newtonian $1/r^2$ case. On a less elementary level, it can be used to discuss the notion of verticality. It also provides a good opportunity to introduce simple plotting tools like those included in python. Finally, it provides a result that may be surprising: Inside flattened rotating bodies modelled as a McLaurin spheroid, gravity tunnels have no exit.

ACKNOWLEDGMENTS

The authors gratefully acknowledge Loïc Villain and Marie-Élizabeth Maury for their encouragements during this work. The authors also thank the anonymous referees for their very helpful suggestions.

APPENDIX: GRAVITATIONAL FIELD INSIDE A MCLAURIN SPHEROID

There are several ways to compute the gravitational fields inside a homogeneous spheroid of density ρ. Here, we follow the approach detailed in Ref. 21. In the frame of the spheroid, its surface is described by

$$\frac{x_s^2}{a^2} + \frac{y_s^2}{a^2} + \frac{z_s^2}{b^2} = 1. \tag{A1}$$

We compute the gravitational potential at a point $P(x_0, y_0, z_0)$ located inside, and we introduce spherical coordinates r, θ, ϕ centered on this point. Any point has rectangular coordinates

$$\begin{cases} x = x_0 + r\sin\theta\cos\phi \\ y = y_0 + r\sin\theta\sin\phi \\ z = z_0 + r\cos\theta. \end{cases}$$

The gravitational potential at P is

$$V(x_0, y_0, z_0) = G\rho \iiint \frac{dV}{r} = G\rho \int_0^{2\pi} d\phi \int_0^{\pi} \sin\theta\, d\theta \int_0^{r_m} r\, dr.$$

Integration over r leads to

$$V(x_0,y_0,z_0)=\frac{G\rho}{2}\int_0^{2\pi}d\phi\int_0^{\pi}\sin\theta\, r_m^2\, d\theta, \tag{A2}$$

where r_m, the maximum value of r, is obtained as a function of θ and ϕ from Eq. (A1)

$$\frac{(x_0+r_m\sin\theta\cos\phi)^2}{a^2}+\frac{(y_0+r_m\sin\theta\sin\phi)^2}{a^2}+\frac{(z_0+r_m\cos\theta)^2}{b^2}=1.$$

Solving for r_m gives

$$r_m=\frac{-B+\sqrt{B^2-AC}}{A},$$

where

$$A(\theta)=\frac{\sin^2\theta}{a^2}+\frac{\cos^2\theta}{b^2}$$
$$B(\theta,\phi)=\frac{x_0\sin\theta\cos\phi}{a^2}+\frac{y_0\sin\theta\sin\phi}{a^2}+\frac{z_0\cos\theta}{b^2}$$
$$C=\frac{x_0^2}{a^2}+\frac{y_0^2}{a^2}+\frac{z_0^2}{b^2}-1.$$

Thus, Eq. (A2) gives

$$V(x_0,y_0,z_0)=\frac{G\rho}{2}\int_0^{2\pi}d\phi\times\int_0^{\pi}\sin\theta\left(\frac{2B^2-AC-2B\sqrt{B^2-AC}}{A^2}\right)d\theta. \tag{A3}$$

This integral involves a quadratic form in x_0, y_0 and z_0. By examination of the symmetries of the problem, it is found that the $2B\sqrt{B^2-AC}$ term contributes to zero (consider antipodal contributions $\theta\to\pi-\theta$ and $\phi\to\phi+\pi$) and that the cross-terms proportional to x_0y_0, x_0z_0 and y_0z_0 must vanish too, leaving us with

$$V(x_0,y_0,z_0)=V_0+\frac{1}{2}\omega_1^2x_0^2+\frac{1}{2}\omega_1^2y_0^2+\frac{1}{2}\omega_2^2z_0^2, \tag{A4}$$

where V_0, ω_1, and ω_2 are constants (they do not depend on x_0, y_0 and z_0). They involve integrals over angular coordinates θ and ϕ. We first focus on ω_1, given by

$$\frac{1}{2}\omega_1^2=\frac{G\rho}{2}\int_0^{2\pi}d\phi\int_0^{\pi}\sin\theta\left[\frac{2\sin^2\theta\cos^2\phi}{a^4A^2(\theta)}-\frac{1}{a^2A(\theta)}\right]d\theta.$$

Integration over ϕ is straightforward

$$\frac{1}{2}\omega_1^2=\frac{\pi G\rho}{a^4}\int_{-\pi/2}^{\pi/2}\sin\theta\left[\frac{\sin^2\theta}{A^2(\theta)}-\frac{a^2}{A(\theta)}\right]d\theta$$

introducing $\lambda\equiv\cos\theta$ and using the relation $b^2=(1-e^2)a^2$, we notice that

$$A(\theta)=\frac{1-\lambda^2}{a^2}+\frac{\lambda^2}{a^2(1-e^2)}=\frac{1}{a^2}\left(1+\frac{e^2\lambda^2}{1-e^2}\right)$$

we arrive at

$$\frac{1}{2}\omega_1^2=-\pi G\rho\int_{-1}^{1}\left[\frac{1-\lambda^2-\left(1+\frac{e^2\lambda^2}{1-e^2}\right)}{\left(1+\frac{e^2\lambda^2}{1-e^2}\right)^2}\right]d\lambda$$
$$\frac{1}{2}\omega_1^2=\frac{\pi G\rho}{1-e^2}\int_{-1}^{1}\frac{\lambda^2\,d\lambda}{\left(1+\frac{e^2\lambda^2}{1-e^2}\right)^2}.$$

Using the property

$$\int_{-1}^{1}\frac{u^2}{(1+c^2u^2)^2}du=\frac{\arctan(c)}{c^3}-\frac{1}{c^2+c^4}, \tag{A5}$$

we find

$$\frac{1}{2}\omega_1^2=\pi G\rho\left[\frac{\sqrt{1-e^2}}{e^3}\arctan\left(\frac{e}{\sqrt{1-e^2}}\right)-\frac{1-e^2}{e^2}\right]$$

which may be rewritten as, using the properties of trigonometric functions, as

$$\boxed{\frac{1}{2}\omega_1^2=\pi G\rho\left[\frac{\sqrt{1-e^2}}{e^3}\arcsin(e)-\frac{1-e^2}{e^2}\right].}$$

Similarly, for ω_2 we have

$$\frac{1}{2}\omega_2^2=\frac{G\rho}{2}\int_0^{2\pi}d\phi\int_0^{\pi}\cos\theta\left[\frac{2\cos^2\theta}{b^4A^2(\theta)}-\frac{1}{b^2A(\theta)}\right]d\theta$$

We integrate over ϕ,

$$\frac{1}{2}\omega_2^2=\frac{\pi G\rho}{b^4}\int_0^{\pi}\cos\theta\left[\frac{2\cos^2\theta}{A^2(\theta)}-\frac{b^2}{A(\theta)}\right]d\theta$$

and we introduce $\lambda=\cos\theta$ to get

$$\frac{1}{2}\omega_2^2=-\frac{a^4\pi G\rho}{b^4}\int_{-1}^{1}\left[\frac{2\lambda^2-\frac{b^2}{a^2}\left(1+\frac{e^2\lambda^2}{1-e^2}\right)}{\left(1+\frac{e^2\lambda^2}{1-e^2}\right)^2}\right]d\lambda$$
$$\frac{1}{2}\omega_2^2=\frac{\pi G\rho}{(1-e^2)^2}\int_{-1}^{1}\left[\frac{1-e^2-\lambda^2(2-e^2)}{\left(1+\frac{e^2\lambda^2}{1-e^2}\right)^2}\right]d\lambda.$$

Using Eq. (A5) and

$$\int_{-1}^{1}\frac{1}{(1+c^2u^2)^2}du=\frac{\arctan(c)}{c}+\frac{1}{1+c^2}, \tag{A6}$$

we then obtain

$$\boxed{\frac{1}{2}\omega_2^2 = \pi G\rho\left[\frac{2}{e^2} - \frac{2\sqrt{1-e^2}}{e^3}\arcsin(e)\right].}$$

The potential is of the form Eq. (A4), which gives the gravitational field of Eq. (2) with ω_1 and ω_2 given in Eq. (3)

The isopotential surfaces are spheroids with ellipticities different from that of the gravitating body. When the body is rotating around the z axis with angular velocity Ω, the potential in the rotating frame is, taking into account the centrifugal potential,

$$V(x_0, y_0, z_0) = V_0 + \left(\frac{1}{2}\omega_1^2 - \frac{1}{2}\Omega^2\right)x_0^2 + \left(\frac{1}{2}\omega_1^2 - \frac{1}{2}\Omega^2\right)y_0^2 + \frac{1}{2}\omega_2^2 z_0^2.$$

The surface of the gravitating body can be an isopotential surface, provided that

$$\frac{\omega_1^2 - \Omega^2}{\omega_2^2} = \frac{b^2}{a^2} = 1 - e^2.$$

The rotating spheroidal body is at equilibrium if Ω is related to e through

$$\Omega^2 = \omega_1^2 - \omega_2^2(1-e^2) = \pi G\rho\left\{\frac{\sqrt{1-e^2}}{e^3}(6-4e^2)\,\mathrm{asin}\,e - \frac{6(1-e^2)}{e^2}\right\}$$

which is relation (4).

[a]Electronic mail: taillet@lapth.cnrs.fr

[1]Edwin H. Hall, "Do falling bodies move south? (part I)," Phys. Rev. **7**, 179–190 (1903).
[2]Angus Armitage, "The deviation of falling bodies," Ann. Sci. **5**, 342–351 (1947).
[3]Harold L. Burstyn, "The deflecting force of the earth's rotation from Galileo to Newton," Ann. Sci. **21**, 47–80 (1965).
[4]A. P. French, "The deflection of falling objects," Am. J. Phys. **52**, 199 (1984).
[5]John F. Wild, "Simple non-coriolis treatments for explaining terrestrial east-west deflections," Am. J. Phys. **41**, 1057–1059 (1973).
[6]Pirooz Mohazzabi, "Free fall and angular momentum," Am. J. Phys. **67**, 1017–1020 (1999).
[7]Jacques Renault and Emile Okal, "Investigating the physical nature of the Coriolis effects in the fixed frame," Am. J. Phys. **45**, 631–633 (1977).
[8]J. M. Potgieter, "An exact solution for the horizontal deflection of a falling object," Am. J. Phys. **51**, 257–258 (1983).
[9]E. Belorizky and J. Sivardière, "Comments on the horizontal deflection of a falling object," Am. J. Phys. **55**, 1103–1104 (1987).
[10]Martin S. Tiersten and Harry Soodak, "Dropped objects and other motions relative to the noninertial earth," Am. J. Phys. **68**, 129–138 (2000).
[11]A. J. Simoson, "Falling down a hole through the Earth," Math. Mag. **77**, 171–189 (2004).
[12]Alexander R. Klot, "The gravity tunnel in a non-uniform Earth," Am. J. Phys. **83**, 231–237 (2015).
[13]Markus Selmke, "A note on the history of gravity tunnels," Am. J. Phys. **86**, 153 (2018).
[14]P. W. Cooper, "Through the Earth in forty minutes," Am. J. Phys. **34**, 68–70 (1966).
[15]Chandrasekhar, "Ellipsoidal figures of equilibrium—An historical account," Com. Pure Appl. Math. **XX**, 251–265 (1967).
[16]See, for instance, John L. Greenberg, *The Problem of the Earth's Shape from Newton to Clairaut* (Cambridge U.P., New York, 1995) for an historical account up to the 18th century.
[17]S. Chandrasekhar, *Ellipsoidal Figures of Equilibrium* (Yale U.P., New Haven, 1969).
[18]The value adopted for the Krasovskyi spheroid, used in geodesy, is $e = 0.0818$, see V. N. Gan'shin, Geometria zemnogo ellipsoida, (Moskva : Izd-vo Nedra, 1967); Geometry of the Earth Ellipsoid (English translation), by J. M. Willis, ACIC-TC-1473, Aeronautical Chart and Information Center (St. Louis, 1969).
[19]Isaac Newton, Philosophiae Naturalis Principia Mathematica, Book III, 3rd ed. (1726). English translation by I. Bernard Cohen and Anne Whitman (University of California Press, Oakland, 1999).
[20]Edward A. Desloge, "Horizontal deflection of a falling object," Am. J. Phys. **53**, 581–582 (1985).
[21]Forest Ray Moulton, *An Introduction to Celestial Mechanics*, 2nd revised ed. (Dover, New York, 1970), republication of the original publication of 1914. See also J. Binney and S. Tremaine, *Galactic Dynamics*, Princeton Series in Astrophysics (Princeton U.P., Princeton, 1987), for a very different derivation of this result.
[22]See Supplementary Material at https://doi.org/10.1119/1.5075716 -006812 for python programs that can be used to plot figures 5 and 8.